

## Modeling and Influence of Shear Retention Parameter on the Response of Reinforced Concrete Structural Elements

L. Dahmani,<sup>a</sup> A. Khennane,<sup>b</sup> and S. Kaci<sup>a</sup>

<sup>a</sup> Mouloud Mammeri University, Tizi-Ouzou, Algeria

<sup>b</sup> University of Southern Queensland, Toowoomba, Australia

УДК 539.4

## Моделирование и оценка влияния ретенционного параметра сдвига на поведение конструктивных элементов из железобетона

Л. Дахмани<sup>а</sup>, А. Хеннане<sup>б</sup>, С. Кази<sup>а</sup>

<sup>а</sup> Университет им. Мулуда Маммери, Тизи-Узу, Алжир

<sup>б</sup> Университет Южного Квинсленда, Тувумба, Австралия

*Для получения полных решений с целью описания равновесия железобетонной конструкции необходимо использовать уравнения, характеризующие физические свойства материала. Изучено поведение железобетонных элементов с учетом изменения ретенционного параметра сдвига (множественной блокировки) и плотности сетки. Постулировалось, что бетон является упругопластическим материалом, для которого справедливы критерий разрушения Друкера–Прагера и закон ассоциированного течения, тогда как стальные элементы арматуры предполагались упруго-идеально-пластичными. Полученные результаты численных расчетов сравнивались с приведенными в литературных источниках.*

**Ключевые слова:** моделирование, армированный бетон, растрескивание, ретенционный параметр сдвига.

**Introduction.** The intact concrete is supposed to be isotropic and linear elastic, while the Rankine criterion is used to detect the crack initiation. In an initially intact integration point, the principal stresses and their directions are evaluated. If the maximum principal stress exceeds the tensile strength, a crack appears in the plane perpendicular to the direction of this stress and the concrete becomes anisotropic [1]. The shearing retention parameter characterizes shear behavior of an element of volume of cracked reinforced concrete. The reduction factor  $\beta$  of the initial rigidity modulus  $G$  is used, in order to take into account a certain redistribution of the shear stress in the cracking plane (aggregate interlock) [2]. The best fit values to be adopted depend on the type of the problem, but the best fit results are obtained if the parameter  $\beta$  values are within the range from 0.3 to 0.5 [2]. In the reinforcement zone, the dowel action can be superimposed with the effect of aggregate interlock, thus conferring a certain rigidity of additional shearing on the crack. The shear retention parameter also depends on the crack opening, and the assessment of its evolution during the loading process becomes complicated if the latter is alternate. In the version of the model used in this work,

various values of  $\beta$  were adopted in order to suitably simulate the reinforced concrete structures [3].

**Compression Model Behavior.** A linear elastic model is used for the reversible part of the strain and an approach based on plasticity with isotropic work hardening is employed for the irreversible part of the strain. The total strain rate is thus broken up into an elastic strain rate  $d\varepsilon^e$  and a plastic strain rate  $d\varepsilon_c^p$  associated to the compression [4, 5],

$$d\varepsilon = d\varepsilon^e + d\varepsilon_c^p \quad (1)$$

or

$$d\sigma = D^e d\varepsilon^e = D^e (d\varepsilon - d\varepsilon_c^p), \quad (2)$$

where  $D^e$  elastic matrix defined by Hooke's law.

The model requires the definition of a load surface which characterizes the plastic criterion, plastic flow rule, work-hardening rule, and collapse condition. The load function for the concrete under a biaxial stress state is generally supposed to depend on two invariants of the stress tensor. A load function of the Drucker-Prager type, which depends on the first invariant of the stress tensor  $I_1$  and the second invariant of the deviatoric stress tensor  $J_2$ , was thus adopted [4]:

$$F = \frac{C\sqrt{J_2} + DI_1}{f_c(K)} - 1 = 0. \quad (3)$$

The experiment has shown that dependence of the load function in  $I_1$  and  $J_2$  gives quite satisfactory results and, moreover, such form simplifies calculation. The constants  $C$  and  $D$  are given as follows:

$$C = \frac{\sqrt{3}(2\mu - 1)}{\mu}, \quad (4)$$

$$D = \frac{\mu - 1}{\mu}, \quad (5)$$

$$\mu = \frac{f_{bc}}{f_c}, \quad (6)$$

where  $f_c$  is compressive strength and  $f_{bc}$  is biaxial compressive strength.

For  $\mu$  we adopt the value of 1.16, according to the experimental results of Kupfer et al. [6, 7].

**Traction Model Behavior.** The two-dimensional behavior of the concrete is based on the Rankine criterion for traction [8]. The evolution of cracking state is taken into account by setting to zero the elastic modulus according to the cracked direction and by the redistribution of the corresponding stresses. The use of a

shearing parameter function of the crack opening in the elasticity matrix of the cracked element makes it possible to simulate the aggregates interlock. Bonds between the concrete and the steel reinforcement are considered to be perfect. The cracked concrete is treated like an orthotropic material, whose orthotropic axes are parallel and normal to the crack direction [9]. The Poisson ratio effect is negligible because of the lack of interaction between the two orthogonal directions after cracking, and the elastic modulus of the concrete normal to the crack direction is reduced to zero.

The total stresses after cracking are given in respect to the axes of local coordinates  $(n, t)$  by

$$\begin{Bmatrix} \sigma_n \\ \sigma_t \\ \tau_{nt} \end{Bmatrix} = \begin{bmatrix} E_b & 0 & 0 \\ 0 & 0 & 0 \\ 0 & 0 & bG \end{bmatrix} \begin{Bmatrix} \varepsilon_n \\ \varepsilon_t \\ \gamma_{nt} \end{Bmatrix} = [D_c] \begin{Bmatrix} \varepsilon_n \\ \varepsilon_t \\ \gamma_{nt} \end{Bmatrix}, \tag{7}$$

where  $E_b$  is elastic modulus of the concrete,  $\beta$  is shear retention parameter of the concrete ( $0 < \beta < 1$ ),  $G$  is shear modulus of the concrete, and  $[D_c]$  is elastic matrix of the cracked element in the local coordinates  $(n, t)$ .

The shear modulus is reduced by shear retention parameter which lies between 0 and 1. In various applications, the value of  $\beta$  is taken equal to 0, when the crack is open, and equal to 1, when the crack is close. This implies that there is no aggregate interlock when the crack is open and a perfect healing when the crack is closed. In order to transform the concrete stresses from local coordinate to global coordinate system (Fig. 1), the following procedure is used

$$[D] = [P]^T [D_c] [P], \tag{8}$$

where

$$[P] = \begin{bmatrix} c^2 & s^2 & cs \\ s^2 & c^2 & -cs \\ -2cs & 2cs & c^2 - s^2 \end{bmatrix}, \tag{9}$$

where

$$c = \cos \psi, \quad s = \sin \psi,$$

$[P]$  is transformation matrix,  $[D]$  is elastic matrix after cracking in the global coordinate  $(X, Y)$ , and  $\psi$  is angle between the crack direction and  $OX$  axis.

The residual stress vector after cracking is given by the following relation:

$$\{\sigma_0\} = \left( [I] - \begin{bmatrix} c^4 & c^2s^2 & 2c^3s \\ c^2s^2 & s^4 & 2cs^3 \\ c^3s & cs^3 & 2c^2s^2 \end{bmatrix} \right) \begin{Bmatrix} \sigma_x \\ \sigma_y \\ \tau_{xy} \end{Bmatrix}, \tag{10}$$

where  $\{\sigma_0\}$  is stress vector adjusted after cracking and  $[I]$  is identity matrix of order  $3 \times 3$ .

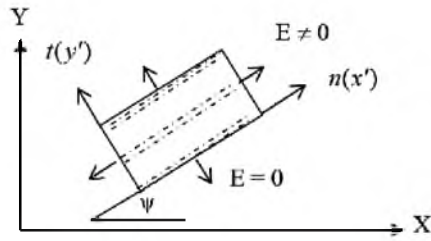


Fig. 1. Representation of smeared crack.

The incremental relation (stress vs strain) in the cracked concrete is given as follows:

$$\{d\sigma\} = [D_c]\{d\varepsilon\}. \quad (11)$$

The total released stresses after cracking will be distributed in the adjacent elements (Fig. 2). The total variation of the stresses will be the following:

$$\{\Delta\sigma\} = \{d\sigma\} - \{\sigma_0\} = [D_c]\{d\varepsilon\} - \{\sigma_0\}, \quad (12)$$

where  $[D_c]$  is elastic matrix of the cracked concrete and  $\{\sigma_0\}$  indicates released stresses after cracking of the concrete.

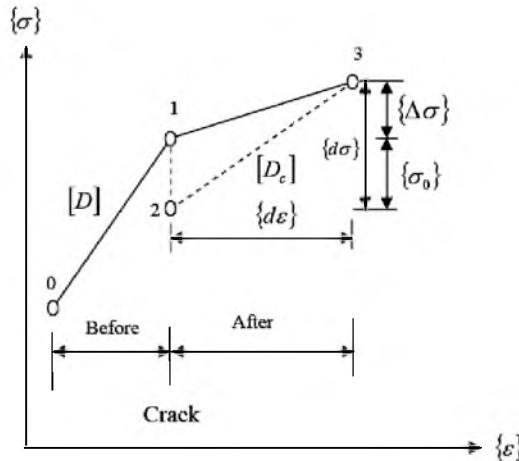


Fig. 2. Stress–strain model of the cracked concrete.

**Nonlinear Calculation Procedure.** The calculation stages are the following:

- (i) introduction of the necessary data for a mesh generation;
- (ii) introduction of the boundary conditions;
- (iii) mesh generation by taking into account the longitudinal and vertical reinforcements;
- (iv) applying a load increment  $\Delta f_i$ ;
- (v) start of the iterative (Newton–Raphson) procedure;
- (vi) evaluation of the residual stress vector  $\{\sigma_0\}$  and the residual force vector  $\{f_0\}$ ;

(vii) calculation of the norm of the residual force vector  $\{f_0\}$ :

1) if the norm of  $\{f_0\}$  is less than the tolerance level, convergence is checked. If the final loading is not reached, apply a new load increment, and repeat the procedure from the step (4);

2) if the norm of  $\{f_0\}$  is greater than the tolerance level, convergence is not checked and if the iteration limit is not reached, repeat the procedure from the step (5);

3) if the maximum iteration is reached, which corresponds to the horizontal stage of the stress–strain curve, and then the load thus found corresponds to the ultimate load;

(viii) posting of the results.

**Validation and Numerical Application Examples.** The model developed for the plane stress calculation of the reinforced concrete structural elements by the finite element method is applied to the study of reinforced concrete panel [9] and a beam [8], where dimensions, reinforcement, and the loading are given in Tables 1 and 2 and illustrated in Figs. 3 and 7, respectively. For reasons of symmetry, only half of the panel and the beam are modeled. Figures 4, 5, 8, and 9 present the response of the elements (panel and beam) in term of the diagram relating the midspan vertical displacements with the applied forces and compare the numerical results with the experimental results. The general pace of the numerical results agrees rather well with the experiment. The refinement of the mesh, as awaited, leads to a more flexible response which approaches the experiment well. In order to appreciate the influence of the shear parameter  $\beta$ , a simulation with various values was carried out. The load–displacement curves obtained are represented (see Figs. 4, 5, 8, and 9) at the same time as the experimental curve. It is noted that the ultimate load is better approached by the values of  $\beta$  between 0.3 and 0.5.

Table 1

Reinforced Concrete Panel [9]

Mechanical property	Concrete	Steel
$E$ (MPa)	20,400	192,000
$\nu$	0.2	0.3
$F_c$ (MPa)	26.7	–
$F_t$ (MPa)	3.4	–
$F_y$ (MPa)	–	360

Table 2

Reinforced Concrete Beam [8]

Mechanical property	Concrete	Steel
$E$ (MPa)	30,000	207,000
$\nu$	0.2	0.3
$F_c$ (MPa)	56	–
$F_t$ (MPa)	6	–
$F_y$ (MPa)	–	320

In order to study the influence of the mesh refinement on the finite element solution, test simulations were carried out with two different meshes: The simulation results are also presented. Figures 6 and 10 show the midspan displacements of the elements for a load of 90 kN for values of shear parameter  $\beta$  ranging from 0 to 1.0. It is noted that for the value of  $\beta$  ranging between 0.3 and 0.5, displacements are almost constant and agree well with the experimental value of 1.6235 mm for the panel and 3.7125 mm for the beam. So one can conclude that the best choice of the shear parameter considerably affects the response of the reinforced concrete structural elements.

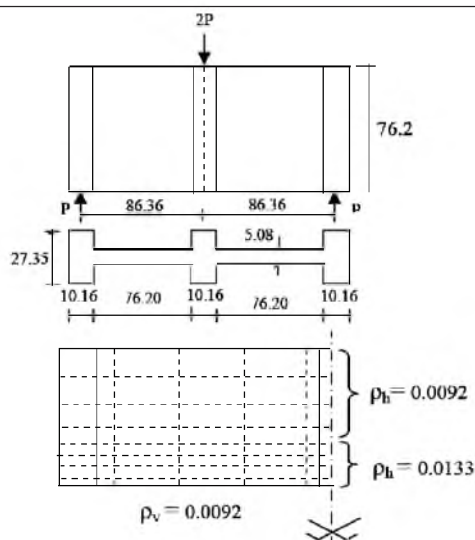


Fig. 3. Geometry, loading, and panel reinforcements. (Dimensions in cm.)

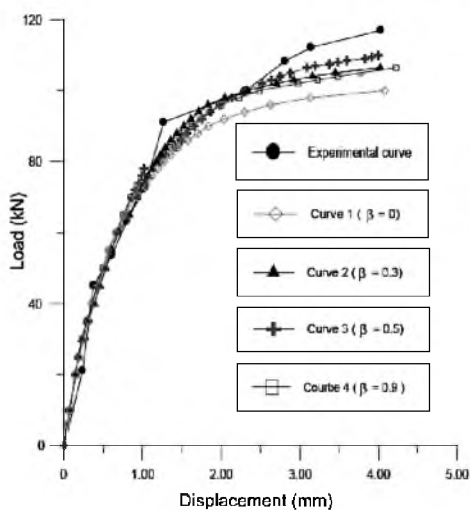


Fig. 4

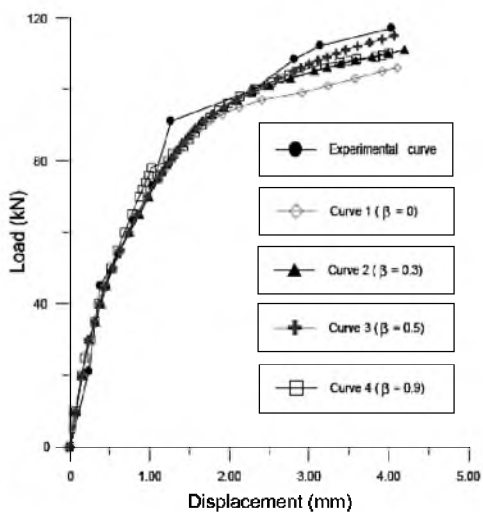


Fig. 5

Fig. 4. Load vs displacement at panel midspan for the different values of  $\beta$  (panel of 20 elements).

Fig. 5. Load vs displacement at panel midspan for the different values of  $\beta$  (panel of 77 elements).

**Influence of Mesh Density.** In finite element modeling, a finer mesh typically results in a more accurate solution. However, as a mesh is made finer, the computation time increases. In order to get a mesh that provides a satisfactory balance between accuracy and computing resources, one way is to perform a mesh convergence study as follows:

1. Create a mesh using the fewest, reasonable number of elements and analyze the model.
2. Recreate the mesh with a denser element distribution, re-analyze it and compare the results to those of the previous mesh.
3. Keep increasing the mesh density and reanalyzing the model until the results converge satisfactorily.

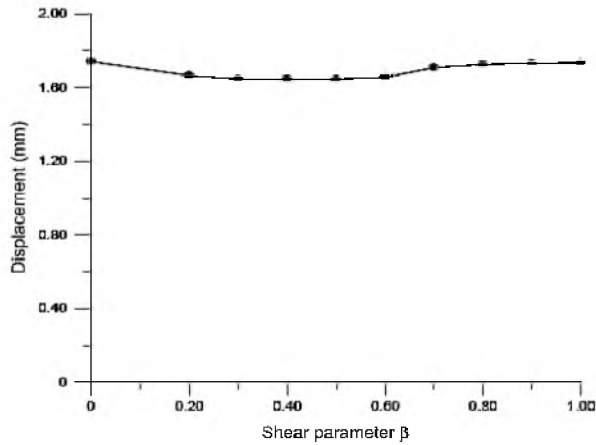


Fig. 6. Displacement at panel midspan for the different values of  $\beta$ .

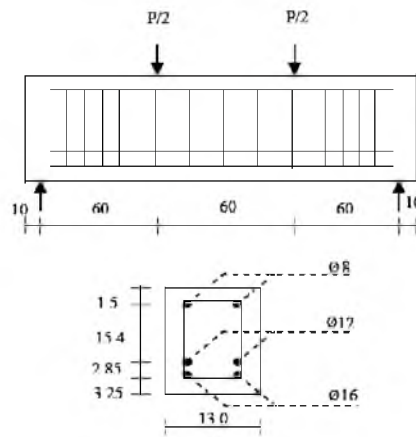


Fig. 7. Geometry, loading, and beam reinforcements. (Dimensions in cm.)

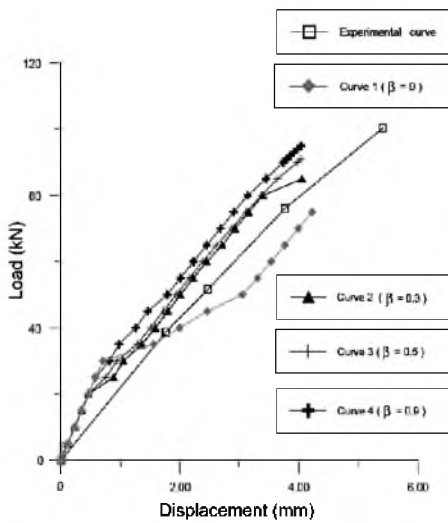


Fig. 8

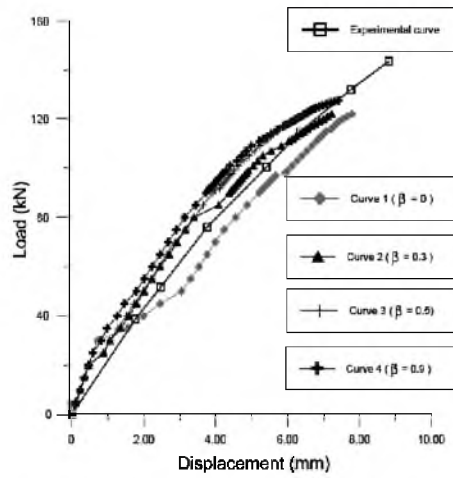


Fig. 9

Fig. 8. Load vs displacement at the beam midspan for the different values of  $\beta$  (panel of 28 elements).

Fig. 9. Load vs displacement at the beam midspan for the different values of  $\beta$  (panel of 60 elements).

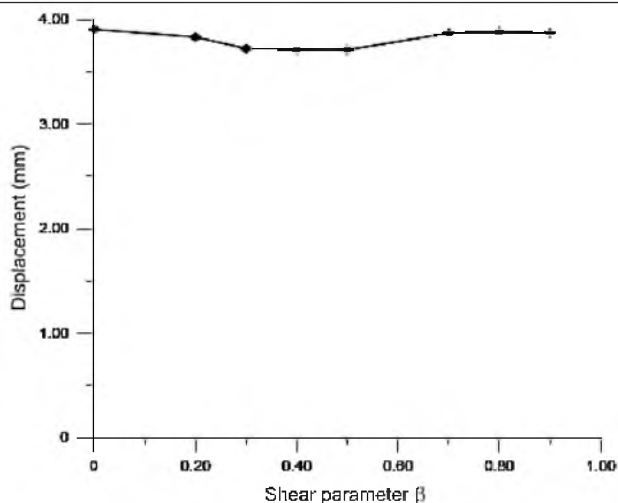


Fig. 10. Displacement at beam midspan for the different values of  $\beta$ .

This type of mesh convergence study provides an accurate solution with a mesh that is sufficiently dense and not overly demanding of computing resources.

Figures 11 and 12 describe the midspan displacement versus the number of elements for the reinforced concrete panel and beam, respectively. The results converge towards the objective value for a grid of 50 elements.

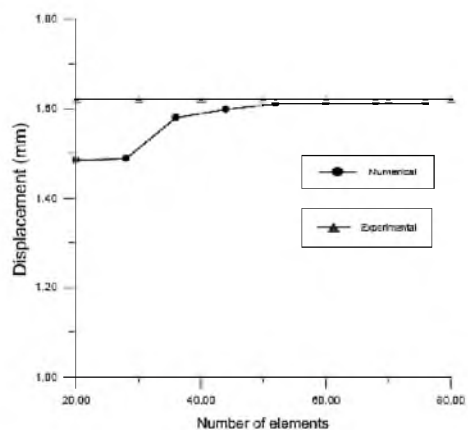


Fig. 11

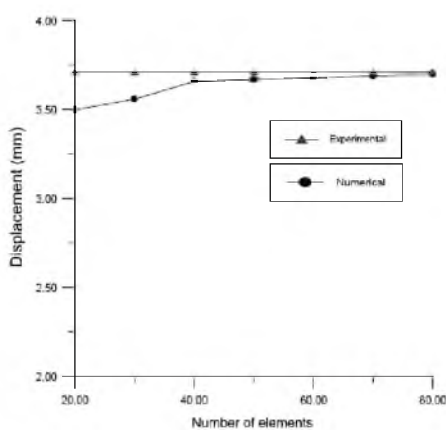


Fig. 12

Fig. 11. Midspan displacement vs number of elements reinforced concrete panel.

Fig. 12. Midspan displacement vs number of elements reinforced concrete beam.

This can be explained by the fact that the isoparametric quadrilateral element used for modeling, reconstitute correctly the deformation required by the beam theory in general.

**Conclusions.** We present a numerical calculation model for evaluation of the response of the reinforced concrete elements under the action of static loads in the elastoplastic field. The results of digital simulation agree well with the experimental results. It is also noted that the best choice of a shear retention



parameter play a significant role in the total response of the structure. The value of  $\beta$  ranging between 0.3 and 0.5 (Fig. 6 and 10) give a better result. The shear parameter used in this model is constant and ranges between 0 and 1.0.

For the future research an improvement can be obtained by introducing a shear retention parameter  $\beta$ , which varies in function of the opening and the closing of the crack, into the model.

## Резюме

Для отримання повних розв'язків із метою опису рівноваги залізобетонної конструкції необхідно використати рівняння, що характеризують фізичні властивості матеріалів. Вивчалася поведінка залізобетонних елементів з урахуванням зміни ретенційного параметра зсуву (множинного блокування) і щільності сітки. Постулювалось, що бетон являє собою пружно-пластичний матеріал, для якого правдиві критерій руйнування Друкера–Прагера та закон асоційованої течії, в той час як сталі елементи арматури припускалися пружно-ідеально-пластичними. Отримані результати числових розрахунків порівнювалися з наведеними у літературних джерелах.

1. Z. P. Bazant and S. S. Kim, "Plastic fracturing theory of concrete," in: *J. Eng. Mech. Div. ASCE*, **105**, No. EM3, June, Proc. Paper 14653, pp. 407–428.
2. W. F. Chen and D. J. Han, *Plasticity for Structural Engineers*, Springer-Verlag, New York (1988).
3. K. Mourad, *Analyse par Éléments Finis des Panneaux en Béton Armé*, Thèse de Magister, Département de Génie Civil, Université Mouloud Mammeri de Tizi-Ouzou (2000).
4. D. C. Drucker and W. Prager, "Soil mechanics and plastic analysis gold limit design," *Quart. Appl. Math.*, **10**, 157–165 (1952).
5. Y. R. Rashid, "Analysis of prestressed concrete nuclear reactor structures," in: Unpublished notes presented at Conference on Prestressed Concrete Nuclear Reactor Structures, University of California, Berkley (1968).
6. H. B. Kupfer and K. H. Gerstle, "Behaviour of concrete under biaxial stresses," *Newspaper Eng. Mech. Div. (ASCE)*, **99**, No. 4, 853–866 (1973).
7. H. Kupfer, H. K. Hilsdorf, and H. Rusch, "Behaviour of concrete under biaxial stresses," *Int. Newspaper*, Aug., 656–666 (1969).
8. D. Ngo, and A. C. Scordelis, "Finite element analysis of reinforced concrete beams," *Newspaper Amer. Concrete Inst.*, **54**, No. 3, 152–163 (1967).
9. V. Cervenka and R. Pulk, "Computer models of concrete structures," *Struct. Int. Eng. (IABSI)*, **2**, 103–107 (1992).

Received 12. 09. 2007